

# The study on elliptical flange hole forming based on finite element analysis

Jiansheng Xia<sup>1, 2\*</sup>, Shasha Dou<sup>1, 2</sup>

<sup>1</sup>Yancheng Institute Of Technology, Yancheng City, Jiangsu Province, China, 224051

<sup>2</sup>Nanjing University of Aeronautics & Astronautics, Nanjing City, Jiangsu Province, China, 211106

Received 1 September 2014, www.cmmt.lv

## Abstract

The flange hole forming is a complex process, Under the assumption of Prandtl-Reuss flow rule and von Mises yield criterion, the incremental elasto-plastic large deformation finite element model was established based on the Updated Lagrangian Formulation (ULF). The elasto-plastic conversions of boundary and deformation are reduced with r-min rule. The friction phenomenon of slippage and viscosity at the boundary interface is revised with increment of revision Coulomb rule. The increment rules are led into the whole stiffness matrix, and derived out the stiffness equation. The studies show that the influence on steel elliptical hole flange forming deformation is influenced by punch structure and parameter. The dates show that finite element simulation and experimental result have a good consistency.

*Keywords:* elasto-plastic, FEM Simulation, elliptical hole flange

## 1 Introduction

Sheet metal forming is a common material processing method, which can be divided into stretching, bending, drawing and flanging, etc. [1]. Its parts can be used in automotive, stationery manufacturing, household appliances industry, when provided with the support group or for pipeline connection and other purposes.

The manufacturing process is using the elliptical punch to stretch forming the sheet, and the blank will bend along the punch radius to form an elliptical shape hole. The hole expands with the dropping of the punch, and the thickness near the hole will gradually thinning, and result the neck and cracked phenomenon. Therefore, if using the finite element to analysis the flange forming process, instead of the trial and error method which are used in general mold factory, it will reduce the costs and shorten development time away [2].

Tang [3] studied the different punches to analyse the distribution of stress and strain in the flange forming with the shell theory and ignoring the bending effect.

Huang and Chen [4,5] investigated the flange hole shape with the different punch radius and shapes. The results show there is the linear relationship between the initial diameter and after stretching.

Takuda and Hatta [6,7] used the rigid-plastic finite element to simulate the sheet metal forming and used ductile fracture criterion to predict zirconium sheet stretch forming limit. The results show that the extension of zirconium sheet is high, but the stretch is low.

Leu [8] studied the numerical analysis and experiment of flange process with the incremental elastic-plastic finite

element method. The results can effectively predict the forming process: when hardening index and orthogonal anisotropy increased, the maximum hole expansion ratio also increased.

Huang and Chien [9] studied the forming process of the flange hole with the frusto-conical punches and different radius, and found the frusto-conical taper punch radius does not affect the forming, the maximum load decreases with the punch radius increasing.

In this paper, the steel sheet SPCC is analysed with the finite element method, some relationships are studied, such us: relationship between punch load and displacement, distribution of stress and strain, distribution of thickness, and verify by actual experiments. It used to reference for operation process and altered design.

## 2 Fundamental theory

### 2.1 VIRTUAL WORK PRINCIPLE

It describes the elastic-plastic deformation with the updated Lagrangian formulation ULF [6], the Virtual work principle formulation can be shown as follows:

$$\int_{V^E} (\ddot{\sigma}_{ij} - e\sigma_{ik}\dot{\epsilon}_{kj})\delta\dot{\epsilon}_{ij}dV + \int_{V^E} \sigma_{jk}L_{ik}\delta L_{ij}dV = \int_{S_f} \dot{f}\delta v_i dS, (1)$$

where,  $\ddot{\sigma}_{ij}$  is the Cauchy stress tensor,  $\dot{\epsilon}_{kj}$  is the rate of stress tensor,  $\dot{\epsilon}_{ij}$  is the strain tensor,  $\sigma_{jk}$  is the rate of strain tensor,  $\delta\dot{\epsilon}_{ij}$  is the virtual strain tensor of the point,  $\delta L_{ij}$  is the virtual velocity gradient tensor of the point,  $\delta v_i$  is the

\*Corresponding author e-mail: xiajiansheng@163.com

velocity component,  $\dot{f}$  is surface force component,  $L_{ij}$  is velocity gradient tensor,  $V$  is unit volume,  $S$  is unit surface area.

### 2.2 CONSTITUTIVE RELATION

In preparing the theory of elasto-plasticity, we have made certain assumptions[10]:

- 1) The material is homogeneous and isotropic;
- 2) There is no strain before manufacturing;
- 3) Temperature effect don't consider when manufacturing;
- 4) It obeys the laws of the Hooke's Law in elastic stage;
- 5) It obeys the von Mises yield rule and Prandtl-Reuss plastic flow rule;
- 6) It contains Isotropic strain hardening in constitutive equation;
- 7) There are elastic strain stage and plastic strain stage in material strain rate;
- 8) Punch, die and holder are steel structure;
- 9) The Bauschinger effect don't consider in reverse unloading.

Taking into account mentioned above, the constitutive relation can be written as follows:

$$\overset{\circ}{\sigma}_{ij} = C_{ijmn}^{ep} \dot{\varepsilon}_{mn}, \tag{2}$$

$$C_{ijmn}^{ep} = C_{ijmn}^e - \frac{C_{ijkl}^e C_{uv}^e \frac{\partial f}{\partial \sigma_{kl}} \frac{\partial f}{\partial \sigma_{uv}}}{C_{kluv}^e \frac{\partial f}{\partial \sigma_{kl}} \frac{\partial f}{\partial \sigma_{uv}} + H' \frac{\sigma_{uv}}{\bar{\sigma}} \frac{\partial f}{\partial \sigma_{uv}}}, \tag{3}$$

where:  $\overset{\circ}{\sigma}_{ij}$  is Jaumann differential of  $\sigma_{ij}$ ,  $C_{ijmn}^{ep}$  is the elastic-plastic module,  $C_{ijmn}^e$  is Elastic module,  $f$  is the initial yield function,  $H'$  is the strain hardening rate,  $\bar{\sigma}$  is Von Mises yield function, so the Matrix form of  $C_{ijmn}^{ep}$  can be expressed as below:

$$[C^{ep}] = [C^e] - \frac{1}{S} \begin{bmatrix} S_1^2 & S_1 S_2 & S_1 S_3 & S_1 S_4 & S_1 S_5 & S_1 S_6 \\ & S_2^2 & S_2 S_3 & S_2 S_4 & S_2 S_5 & S_2 S_6 \\ & & S_3^2 & S_3 S_4 & S_3 S_5 & S_3 S_6 \\ & & & S_4^2 & S_4 S_5 & S_4 S_6 \\ & & & & S_5^2 & S_5 S_6 \\ & & & & & S_6^2 \end{bmatrix}, \tag{4}$$

where,

$$S = \frac{4}{9} \bar{\sigma}^2 H' + S_1 \sigma'_{xx} + S_2 \sigma'_{yy} + S_3 \sigma'_{zz} + 2S_4 \sigma'_{yz} + 2S_5 \sigma'_{zx} + 2S_6 \sigma'_{xy}, \tag{5}$$

$$S_1 = 2G\sigma'_{xx}, S_2 = 2G\sigma'_{yy}, S_3 = 2G\sigma'_{zz}, \tag{6}$$

$$S_4 = 2G\sigma'_{yz}, S_5 = 2G\sigma'_{zx}, S_6 = 2G\sigma'_{xy}, \tag{7}$$

where  $\sigma'_{ij}$  is deviator of  $\sigma_{ij}$ ,  $G$  is the friction flow potential,  $G = \sigma_1^2 + \sigma_2^2$ ,  $[C^e]$  is the equation in minimum strain, which can be expressed as below:

$$[C^e] = \frac{E}{1+\nu} \begin{bmatrix} \frac{1-\nu}{1-2\nu} & \frac{1-\nu}{1-2\nu} & \frac{1-\nu}{1-2\nu} & 0 & 0 & 0 \\ & \frac{1-\nu}{1-2\nu} & \frac{1-\nu}{1-2\nu} & 0 & 0 & 0 \\ & & \frac{1-\nu}{1-2\nu} & 0 & 0 & 0 \\ & & & \frac{1}{2} & 0 & 0 \\ & & & & \frac{1}{2} & 0 \\ & & & & & \frac{1}{2} \end{bmatrix}, \tag{8}$$

*symm*

where,  $E$  is modulus of elasticity,  $\nu$  is Poisson's ratio. If the material is homogeneous and isotropic, the Elasto-plastic rate equation can be written:

$$\overset{\circ}{\sigma}_{ij} = \frac{E}{1+\nu} \left[ \delta_{ik} \delta_{jl} + \frac{\nu}{1-2\nu} \delta_{ij} \delta_{kl} - \frac{3\alpha \left( \frac{E}{1+\nu} \right) \sigma'_{ij} \sigma'_{kl}}{2\bar{\sigma}^2 \left( \frac{2}{3} H' + \frac{E}{1+\nu} \right)} \right] \dot{\varepsilon}_{kl}. \tag{9}$$

When  $\alpha = 1$ , it is a plastic stage; when  $\alpha = 0$ , it is an elastic stage or unloading stage.

Equivalent stress and equivalent plastic strain relations can express by  $n$ -power law equation:

$$\dot{\sigma} = C (\varepsilon_0 + \dot{\varepsilon}_p)^n, \tag{10}$$

where:  $C$  is material constant,  $n$  is strain hardening index;  $\dot{\sigma}$  is the equivalent stress,  $\dot{\varepsilon}_p$  is the equivalent plastic strain,  $\varepsilon_0$  is the initial strain.

### 2.3 THE FINITE ELEMENT FORMULA

Finite element analysis is the method that the structure is divided into many small units called discrete entity. Based on Large deformation stress and stress rate relation, the finite deformation of Update Lagrangian Formulation, material constitution relationship, the velocity distribution of each unit is shown below:

$$\{v\} = [N] \{\dot{d}\}, \tag{11}$$

$$\{\dot{\varepsilon}\} = [B] \{\dot{d}\}, \tag{12}$$

$$\{L\} = [M]\{\dot{d}\}, \tag{13}$$

where  $[N]$  is shape function,  $\{\dot{d}\}$  is nodal velocity,  $[B]$  is strain rate-velocity matrix,  $[M]$  is velocity gradient-velocity matrix.

The principle of virtual work equation and the constitutive equation based on update Lagrangian is linear equation. The equation can be written by the form of incremental representation.

After finite element discrimination, the large deformation rigid general equation is written as below:

$$[K]\{\Delta u\} = \{\Delta F\}, \tag{14}$$

where:

$$[K] = \sum_{(E)} \int_{V^e} [B]^T ([C^{ep}] - [Q])[B] dV + \sum_{(E)} \int_{V^e} [E]^T, \tag{15}$$

$$\{\Delta F\} = \sum_{(E)} \int_{S^e} [N]^T \{\dot{f}\} dS \Delta t, \tag{16}$$

$[K]$  is the overall Elasto-plastic stiffness matrix,  $\{\Delta F\}$  is the nodal displacement increment,  $\{\Delta u\}$  is the nodal forces incremental,  $[Q]$  and  $[Z]$  are stress correction matrix.

$$Q = \begin{bmatrix} 2\sigma_{xx} & 0 & 0 & \sigma_{xy} & 0 & \sigma_{xz} \\ & 2\sigma_{yy} & 0 & \sigma_{xy} & \sigma_{zy} & 0 \\ & & 2\sigma_{zz} & 0 & \sigma_{zy} & \sigma_{xz} \\ & & & \frac{1}{2}(\sigma_{xx} + \sigma_{yy}) & \frac{1}{2}(\sigma_{zx}) & \frac{1}{2}(\sigma_{zy}) \\ & & & & \frac{1}{2}(\sigma_{yy} + \sigma_{zz}) & \frac{1}{2}(\sigma_{xy}) \\ & & & & & \frac{1}{2}(\sigma_{xx} + \sigma_{zz}) \end{bmatrix}, \tag{17}$$

*symm*

$$Z = \begin{bmatrix} \sigma_{xx} & 0 & 0 & \sigma_{xy} & \sigma_{xz} & 0 & 0 & 0 & 0 \\ & \sigma_{yy} & 0 & 0 & 0 & \sigma_{xy} & \sigma_{yz} & 0 & 0 \\ & & \sigma_{zz} & 0 & 0 & 0 & 0 & \sigma_{xz} & \sigma_{yz} \\ & & & \sigma_{yy} & \sigma_{yz} & 0 & 0 & 0 & 0 \\ & & & & \sigma_{zz} & 0 & 0 & 0 & 0 \\ & & & & & \sigma_{xx} & \sigma_{xz} & 0 & 0 \\ & & & & & & \sigma_{zz} & 0 & 0 \\ & & & & & & & \sigma_{xx} & \sigma_{xy} \\ & & & & & & & & \sigma_{yy} \end{bmatrix}. \tag{18}$$

*symm*

### 2.4 FRICTION PROCESSING

There is friction in sheet forming process, so we need to pay attention to materials and tools of the interface conditions [11]. When the material moves along the tool surface curve of the slide, the contact force can be expressed as:

$$F = F_l l + F_n n, \tag{19}$$

where,  $F_l$  is radial force and  $F_n$  is normal force, and differential equation of  $F$  can be expressed as:

$$\dot{F} = \dot{F}_l l + F_l \dot{l} + \dot{F}_n n + F_n \dot{n}, \tag{20}$$

where, differentials of  $l$  and  $n$  are expressed as:

$$\dot{l} = -\Delta u_l^{rel} / R, \tag{21}$$

$$\dot{n} = \Delta u_l^{rel} / R, \tag{22}$$

where,  $R$  is tool radius,  $\Delta u_l^{rel}$  is the local relative velocity between the tool and node, and the nodes relative speed can be expressed as:

$$\Delta u_l^{rel} = \Delta u_l - \dot{u}_{tool} \sin \theta, \tag{23}$$

where,  $\Delta u_l$  is the contact tangent displacement increment of nodes,  $\dot{u}_{tool}$  is the displacement increment of tooling,  $\theta$  is the rotation angle.

The increment formula of  $\dot{F}$  is expressed as follow:

$$\dot{F} = \left( \dot{F}_l - F_n \Delta u_l / R + F_n \dot{u}_{tool} \sin \theta / R \right) \cdot l + \left( \dot{F}_n - F_l \Delta u_l / R - F_l \dot{u}_{tool} \sin \theta / R \right) \cdot n. \tag{24}$$

Rigid matrix governing equation of the contact nodes is expressed below:

$$\begin{bmatrix} K & \dots \\ \dots & K_{11} + F_n / R & K_{12} \\ \dots & K_{21} + F_n / R & K_{22} \end{bmatrix} \begin{Bmatrix} \dots \\ \Delta u_l \\ \Delta u_n \end{Bmatrix} = \begin{Bmatrix} \dots \\ \dot{F}_l + F_n \dot{u}_{tool} \sin \theta / R \\ \dot{F}_n - F_l \dot{u}_{tool} \sin \theta / R \end{Bmatrix}. \tag{25}$$

2.5 INCREMENTAL STEPS OF  $R_{MIN}$  METHOD

Using the elastic plastic finite element method with large deformation method, also called the Yamada  $r_{min}$  method. Each incremental step value is equal to incremental

displacement of initial deformation increment of the tooling. Adopting the method of updated Lagrangian formulation, calculating each increment of displacement, strain, stress, load, springback value after forming the final shape of sheet metal in unloading condition, the value of load incremental in each step is controlled by  $r_{min}$  formula, which is shown as below:

$$r_{min} = MIN(r_1, r_2, r_3, r_4, r_5), \tag{26}$$

where,  $r_1$  is The maximum allowable strain increment,  $r_2$  is the maximum allowable rotation increment,  $r_3$  is the minimum value in all elastic elements,  $r_4$  is contact position between free node and tooling,  $r_5$  is discont position between free node and tooling.

3 Numerical analysis flow

Based on the finite deformation theory, ULF equation and  $r_{min}$  method, a set of effective analysis of sheet metal forming process is established. Firstly, a 3d part and mold is designed with the NX software, and then mesh them with NASTRAN software. Secondly, the meshed models are drawn into the data file and did finite element analysis. The simulation flow chart is shown in Figure 1.

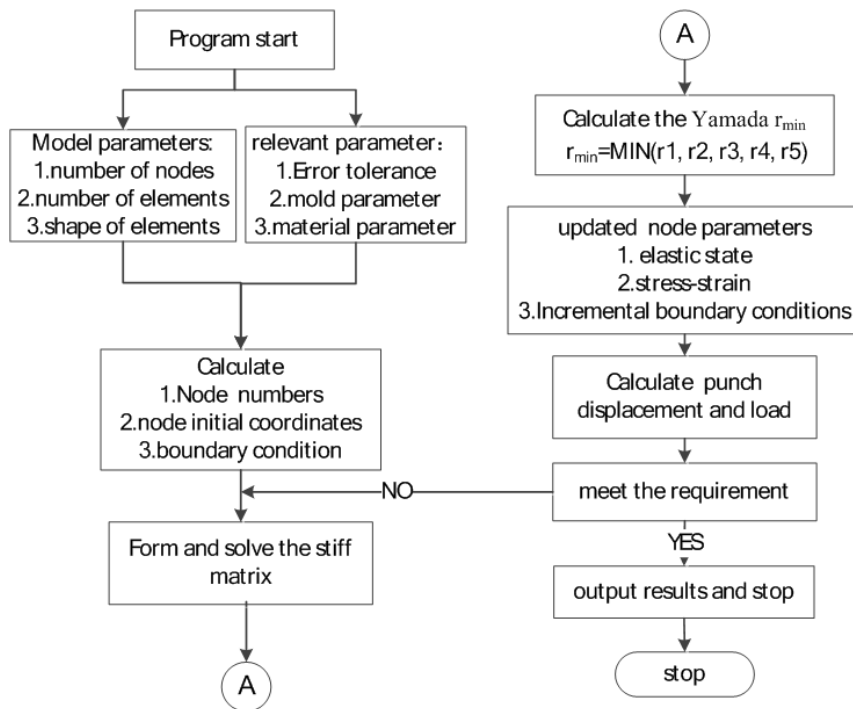


FIGURE 1 Numerical simulation of flow chart

Based on the theory upwards, the research of steel elliptical cup drawing is studied, including relationship between the punch load and displacements, stress and strain, thickness, spring-back and warpage. Simulation experimental parameters were carried out, which are friction coefficient ( $\mu$ ), punch radius ( $r_p$ ), die radius ( $R_d$ ).

The parameters of warpage problems are verified by the experiment are optimized and served a reference for drawing designer.

The whole structure is composed of punch, die and blank holder. The model picture was shown as Figure 2.

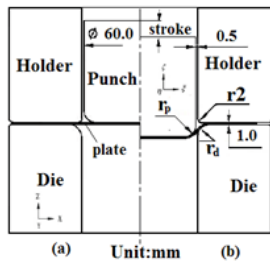


FIGURE 2 Sheet metal and die size chart; (a) before deformation; (b) after deformation

The initial relation of part and die is shown in Figure 2a, also, the punch down a certain travel case is shown Figure 2b. It takes two coordinates to solve the problem, which are fixed coordinates ( $X, Y, Z$ ) and local coordinates ( $\xi, \eta, \zeta$ ). It uses the fixed coordinates ( $X, Y, Z$ ) when nodes do not contact with the tool, and uses the local coordinates ( $\xi, \eta, \zeta$ ) when nodes contact with the tooling. Using coordinates rule based on the right-hand rule.  $L$ -axis is the tangential direction of contact line between the part and tools when  $n$ -axis is the normal direction.

The contact condition of each node of plates will change depending on deformation in sheet metal forming. When the displacement increment is zero, the boundary conditions of increment displacement of the next node will changes to free node boundary conditions. When sheet contacts the tools, contact condition is changed to the boundary conditions, which bases on the generalized  $r_{min}$  method.

Blanks preparation: JIS SPCC steel sheet, cutting into the outer diameter 130.0mm and an initial elliptical hole in the centre of the sheet by CNC, the long axis of elliptical size 23mm, short axis dimension 12mm.

Experimental arrangement: the sheet metals are put on hydro forming machine, the centre of the sheet is consistent with the mold. Set pressure of the pressure 160kN, the punch speed 1.0mm/s. Measured the experimental data of header punch load and the stroke of the punch. Finally, measured and recorded the hole of the flange height was measured with calipers.

JIS SPCC material stainless steels are provided by a china steel Crop, of which the mechanical properties as shown in Table1 as below [12].

TABLE 1 Mechanical properties of JIS SPCC

stress-strain relationship: $\bar{\sigma}=563.64(0.011+\bar{\epsilon}_p)^{0.2781}$	
initial thickness: $t = 0.6\text{mm}$	Poisson's ratio: $\nu=0.3$
yield stress: $\sigma_y=163.5\text{MPa}$	Anisotropy value: $r_0 = 1.71,$ $r_{45} = 1.52, r_{90} = 2.11$
Yang coefficient: $E=2.1 \times 10^5 \text{MPa}$	

Because of the symmetrical sheet model, 1/4 model is taken to analysis.

It uses the quadrilateral segmentation of degenerated shell element in sheet metal meshing, when the die meshing uses the triangle segmentation.

## 4 Results

### 4.1 DISTRIBUTION OF STRESS AND STRAIN

The hole elliptical flange stress distribution as shown in Figure 3. As can be seen from the figure, the stress near the long axis of the hole is maximum, the maximum value is 395MPa, because the holes of the flange forming influences by tensile stress, and the curvature is large near the long axis of the hole, the circumferential stress has concentration phenomenon. Stress near the short axis of the holes gradually decreases in the direction of elliptical, which is due to the short axis of the inner peripheral edge of the blanks curvature of the hole is small, the stress in this area is small, in addition, the stress value is less than the value of stress at the long axis.

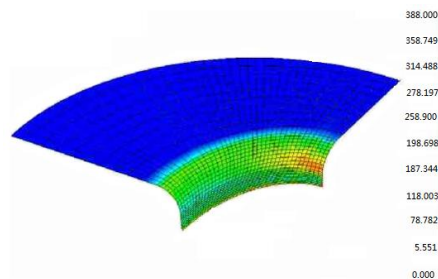


FIGURE 3 The figure of stress distribution

### 4.2 FLANGE HEIGHT ANALYSIS

The compare of heights of elliptical hole flange between numerical analysis and experimental is shown in Figure 4, the measured points from the long axis to short axis along the axis elliptical. As can be seen from the figure, the maximum height position at the short axis. The value is compared with the experimental results, the error is less than 2%.

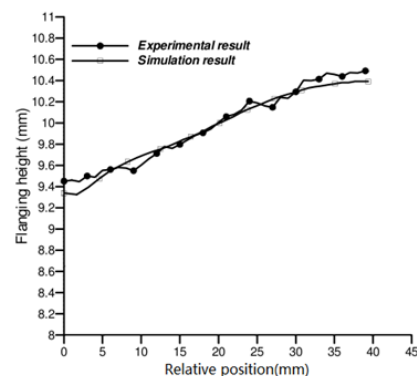
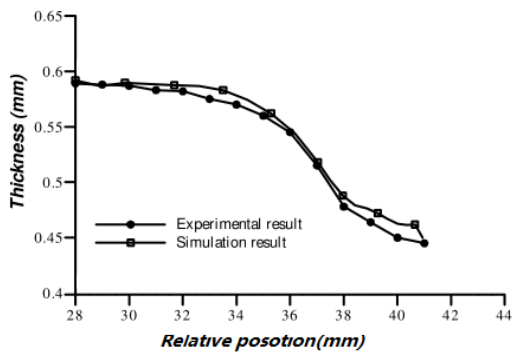


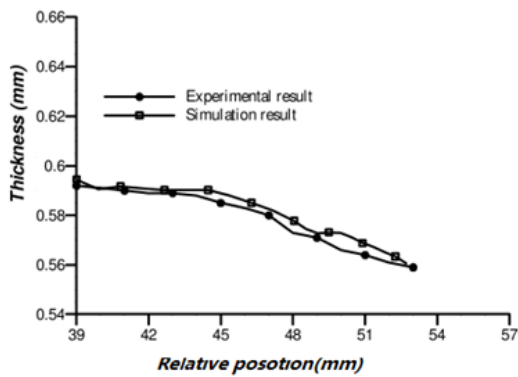
FIGURE 4 The flange height distribution

### 4.3 THICKNESS CHANGE ANALYSIS

The sheet mental is used to do drawing experiment analysis. The thickness data are measure along the direction of long-axis and short-axis and as shown in Figure 5. As can be seen from the Figure 5a.



a) The thickness in long-axis



b) The thickness in short-axis

FIGURE 5 Thickness change analysis in long axis and short axis

Because the part was held by holder and die in this area, the thickness changed a little from the area 0.0mm to 28.0mm. After that area, the thickness is thin gradually, until to the minimum value. The reason is that the sheet is affected by the maximum tensile stress, and the hole becomes larger and the thickness become thin. As can be seen from the Figure 5b), because the part was held by holder and die in this area, the thickness changes a little from the area 0.0mm to 39.0mm. After that area, the thickness is thin gradually, until to the minimum value. However, because the short-axis of curvature and Tensile stress are small, the value also changes a little.

The thinnest thickness is in the bottom area near the long-axis, which is the 0.45mm and slightly larger than the rupture thickness, then the part can be finished.

#### 4.4 FORMING LIMIT ANALYSIS

In order to find out the limit thickness of elliptical flange, some experiments are carried out with the different diameters of sheet, and set the value 0.41mm as the criterion of rupture. If the thickness is thinner, the program will judge that the sheet is in the limit thickness. FR (Forming ratio) LFR (Limit Forming Ratio) and EFR (Excessive Forming Ratio) are referred by Huang and Chien [9].

DR (Drawing Ratio), LDR (Limit Drawing Ratio) and EDR (Excessive Drawing Ratio) are used to calculate and judge, which are defined by Huang [9].

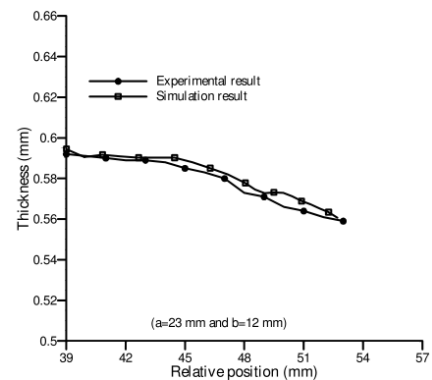
$$FR = \frac{D_p}{D_h} = \frac{C_p}{C_h}, \tag{27}$$

$$LFR = \frac{D_p}{D_{h,min}} = \frac{C_p}{C_{h,min}}, \tag{28}$$

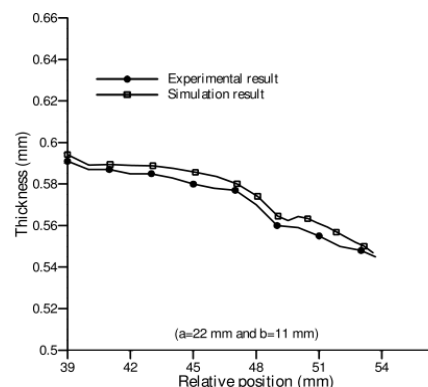
$$EDR = \frac{D_p}{D_{h,f}} = \frac{C_p}{C_{h,f}}, \tag{29}$$

where,  $D_p$  is the diameter of punch;  $D_h$  is the diameter of sheet with necking or fracture;  $D_{h, min}$  is the maximum diameter of sheet without necking or fracture;  $D_p$  is the perimeter of the elliptical punch;  $D_{h,f}$  is the perimeter of the sheet without necking or fracture;  $C_p$  is the circumference of punch,  $C_h$  is the circumference of initial inner elliptical hole with necking or fracture;  $C_{h,min}$  is the maximum the circumference of initial inner elliptical hole without necking or fracture;  $C_{h,f}$  is circumference of initial inner elliptical hole with part necking or fracture. The experimental arrangement is shown in Table 2 and the simulation results are shown as Figure 6. When  $a = 23\text{mm}$   $b = 12\text{mm}$  ( $FR=1.38$ ) and  $a = 22\text{mm}$   $b = 11\text{mm}$  ( $LFR=1.46$ ), the forming complete without necking or rupture. When  $a = 21\text{mm}$   $b = 10\text{mm}$  ( $EFR=1.55$ ), the forming with necking or rupture. So the  $LFR=1.46$  is the limit value.

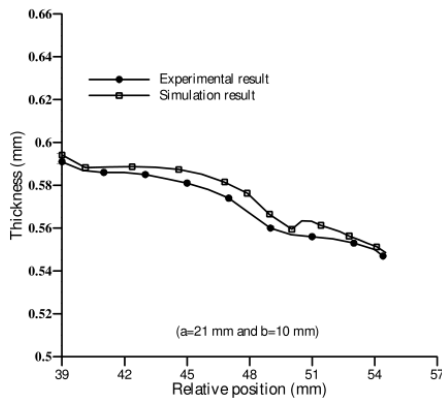
The other experiments were carried out and found the result is closed to the simulation value.



a) thickness distribution when  $FR=1.38$



b) thickness distribution when  $FR=1.46$

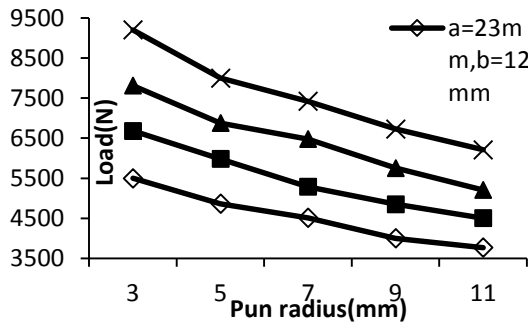


c) thickness distribution when FR=1.38

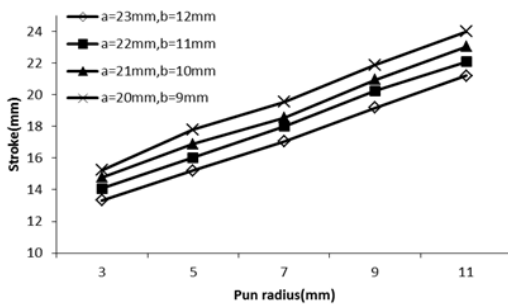
FIGURE 6 The distribution of thickness

TABLE 2 Maximum punch load and stroke with the different radius of punch

Elliptical sizes	A=23mm, b=12mm		A=22mm, b=11mm		A=21mm, b=10mm		A=20mm, b=9mm	
Pun radius	Load(N)	Stroke(mm)	Load(N)	Stroke(mm)	Load(N)	Stroke(mm)	Load(N)	Stroke(mm)
3.0mm	5500	13.32	6680	14.08	7810	14.78	9200	15.23
5.0mm	4865	15.21	5980	16.02	6875	16.89	8000	17.80
7.0mm	4512	17.05	5285	18.01	6476	18.56	7420	19.55
9.0mm	4000	19.18	4850	20.26	5753	20.96	6730	21.89
11.0mm	3770	21.21	4505	22.08	5208	23.05	6210	24.00



a) Load distribution



b) Stroke distribution

FIGURE 7 Load and stroke distribution with the radius of punch

### 4.5 PUNCH RADIUS ANALYSIS

In order to study the relationship between the initial inner elliptical hole and punch or punch radius, five experiments are carried out. The radius of punch and punch fillet are 3.0mm, 5.0mm, 7.0mm, 9.0mm and 11.0mm, respectively. The results are as shown in Table 2 as below.

As can be seen from the Figure 7a, maximum punch load decreases with increasing of punch radius and initial elliptical hole diameter.

As can be seen from the Figure 7b, maximum punch stroke increases with increasing of punch radius and initial elliptical hole diameter.

### 5 Conclusion

Based on the numerical analysis and experimental results, combined with finite element method with the incremental Elasto-plastic theory, analysed Stress distribution, thickness analysis, forming limit analysis and punch radius analysis. It obtains the following conclusions:

1) Maximum stress and minimum thickness values occur in the area of the long-axis of the hole. This is due to the hole withstand greater the tensile stress near the long-axis area, and the tensile stress will make thickness thinner. The thickness changed small in the short-axis, because the curvature and stress are small.

2) In the long-axis, maximum punch load decreases with increasing punch radius and initial elliptical hole diameter.

3) Maximum punch stroke increases with increasing punch radius and decreasing of initial elliptical hole diameter.

4) As the forming limit defined by the inner circumference and diameter of elliptical punch, the experimental flange forming limit ratio of 1.46.

### Acknowledgments

A Project Funded by the Key Laboratory for Advanced Technology in Environmental Protection of Jiangsu Province (AE201039) (AE201038). Natural science foundation of Jiangsu Province (BK2012250). The Natural Science Foundation for General Universities of Jiangsu Province (China). (12KJD520010). The composite processing machine of small and medium-sized aircraft fuselage part (2014ZX04001071).

## References

- [1] Xia J S Dou S S 2013 Experimental Research on the Flanging Height Adjustment Based on Environmental Way *International Journal of Applied Environmental Sciences* **8**(20) 2470-89
- [2] Huang Y M, Chen T C 2005 Influence of Blank Profile on the V-Die Bending Camber Process of Sheet Metal *International Journal of Advanced Manufacturing Technology* **25**(7) 668-77
- [3] Tang S C 1981 Large Elastic-Plastic Strain Analysis of Flanged Hole Forming *Computers & Structures* **13**(1-3) 363-70
- [4] Kumagai T, Saiki H, Meng Y 1999 Hole Flanging with Ironing of Two-Ply Thick Sheet Metals *Journal of Materials Processing Technology* **89-90** 51-7
- [5] Huang Y M, Chen T C 2001 The Formability Limitation of the Hole-Flanging Process *Journal of Materials Processing Technology* **117**(1) 43-51
- [6] Huang Y M, Chien K H 2001 Influence of the Punch Profile on the Limitation of Formability in Hole-Flanging Process *Journal of Materials Processing Technology* **113**(1) 720-4
- [7] Takuda H, Hatta N 1998 Numerical Analysis of Formability of a Commercially Pure Zirconium Sheet in Some Forming Processes *Materials Science and Engineering* **242**(1) 15-21
- [8] Leu D K 1996 Finite-Element Simulation of Hole-Flanging Process of Circular Sheets of Anisotropic Materials *International Journal of Mechanical Sciences* **38**(8) 917-33
- [9] Huang Y M, Chien K H 2002 Influence of Cone Semi-Angle on the Formability Limitation of the Hole-Flanging Process *International Journal of Advanced Manufacturing Technology* **19**(8) 597-606
- [10] Sousa L C, Castro C F, António C A C 2006 Optimal Design of V and U Bending Processes Using Genetic Algorithms *Journal of Material Processing Technology* **172**(1) 35-41
- [11] Liu G, Lin Z, Xu W, Bao Y 2002 Variable Blankholder Force in U-Shaped Part Forming for Elimination Springback Error *Journal of Material Processing Technology* **120**(1-3) 259-64
- [12] Samuel M 2000 Experimental and numerical prediction of springback and side wall curl in u-bending of anisotropic sheet metals *Journal of Materials Processing Technology* **3**(105) 382-93

## Authors



**Jiansheng Xia, born in September, 1980, Yancheng City, Jiangsu Province, P.R. China**

**Current position, grades:** lecturer at Yancheng Institute of Technology, China.

**University studies:** BSc in Mechanical engineering and automation at Northeast Agricultural University in China. MSc at Northeast Agricultural University.

**Scientific interests:** mold design, CAD/CAE/CAM technologies.

**Publications:** more than 10 papers.

**Experience:** teaching experience of 8 years, 2 scientific research projects.



**Shasha Dou, born in December, 1982, Yancheng City, Jiangsu Province, P.R. China**

**Current position, grades:** lecturer of Yancheng Institute of Technology, China.

**University studies:** BSc in mechanical engineering and automation at Shandong University of Technology in China, MSc at Shandong University of Technology.

**Scientific interests:** plastic mold design, CAD/CAE/CAM technologies.

**Publications:** more than 10 papers.

**Experience:** teaching experience of 8 years, 1 scientific research projects.